Synergistic effects of arsenic trioxide combined with ascorbic acid in human osteosarcoma MG-63 cells: a systems biology analysis

X.C. HUANG, X.Y.M. MAIMAITI¹, C.W. HUANG², L. ZHANG³, Z.B. LI, Z.G. CHEN³, X. GAO⁴, T.Y. CHEN³

Rehabilitation Department, Zhongshan Hospital of Fudan University, Shanghai, China ¹Microscope Repairing Surgery Section, the First Affiliated Hospital of Xinjiang Medical University, Xinjiang Uygur Autonomous Region, China

²Medical Department, Zhongshan Hospital of Fudan University, Shanghai, China

Xiaochun Huang and Xiayimaierdan Maimaiti are regarded as co-first author

Abstract. – OBJECTIVE: To further understand the synergistic mechanism of As₂O₃ and asscorbic acid (AA) in human osteosarcoma MG-63 cells by systems biology analysis.

MATERIALS AND METHODS: Human osteosarcoma MG-63 cells were treated by As_2O_3 (1 μ mol/L), AA (62.5 μ mol/L) and combined drugs (1 μ mol/L As_2O_3 plus 62.5 μ mol/L AA). Dynamic morphological characteristics were recorded by Cell-IQ system, and growth rate was calculated. Illumina beadchip assay was used to analyze the differential expression genes in different groups. Synergic effects on differential expression genes (DEGs) were analyzed by mixture linear model and singular value decomposition model. KEGG pathway annotations and GO enrichment analysis were performed to figure out the pathways involved in the synergic effects.

RESULTS: We captured 1987 differential expression genes in combined therapy MG-63 cells. FAT1 gene was significantly upregulated in all three groups, which is a promising drug target as an important tumor suppressor analogue; meanwhile, HIST1H2BD gene was markedly downregulated in the As₂O₃ monotherapy group and the combined therapy group, which was found to be upregulated in prostatic cancer. These two genes might play critical roles in synergetic effects of AA and As₂O₃, although the exact mechanism needs further investigation. KEGG pathway analysis showed many DEGs were related with tight junction, and GO analysis also indicated that DEGs in the combined therapy cells gathered in occluding junction, apical junction complex, cell junction, and tight junction.

CONCLUSIONS: AA potentiates the efficacy of As₂O₃ in MG-63 cells. Systems biology analysis showed the synergic effect on the DEGs.

Key Words:

Arsenic trioxide, Osteosarcoma, Synergistic effect, Systems biology analysis.

Introduction

Osteosarcoma is the most common and aggressive type of bone cancer1, which may not only cause extremity disability, but also threaten life by metastasis. Surgery was the only form of treatment in the pre-chemotherapy era, when the survival rate was less than 20%2. Recently limb salvage surgery with large dose neoadjuvant chemotherapy saves many patients' limbs and lives. However, most of chemotherapeutics, such as ifosfamide, cis-platinum, adriamycin and methotrexate, have a major problem that large dose brings about effectiveness on tumor as well as severe side effects, among which tiredness, nausea, headache, edema, diarrhea and vomit are common ones, and leukocytosis and retinoic acid syndrome are the most severe ones³. Thus, novel therapeutic strategies with less systemic toxicity and higher effectiveness are demanded urgently.

Arsenicals have been used to treat diseases, such as ulcer, haemorrhoids and dysentery, for thousands of years in Chinese traditional medicine⁴. In the recent years arsenic trioxide (As₂O₃) was found to be effective on recurrent acute promyelocytic leukemia (APL, M3)⁵ and solid tumor⁶. More importantly As₂O₃ did not

³Department of Orthopedic Surgery, Zhongshan Hospital of Fudan University, Shanghai, China

⁴Genergy Biotechnology (Shanghai) Co., Ltd, Shangai, China

accumulate in blood plasma or induce myelosuppression in most of the patients. In addition, As_2O_3 inhibits proliferation of osteosarcoma cells in a time-dependent and dose-dependent manner, the inhibition rate can reach 70% when the concentration of As_2O_3 was higher than 1 μ mol/ L^7 . Whereas, arsenic compounds have double-edged effects (anticancer and carcinogenic effects) dependent on dosage⁸. Drug combination could be a valuable way to lower systemic toxicity and increase effectiveness of anticancer drugs such as As_2O_3 .

Ascorbic acid (AA) has antioxidative effects, which can decrease reduced glutathione with no toxicity itself. Previous researches9 have found AA enhanced anticancer activity of As₂O₃; AA had sensitization effect on apoptosis-inducing activity of As₂O₃ in human multiple myeloma RP-MI8226 cells, which depended on overexpression of death receptor 4 (DR4)10; AA enhanced cytotoxicity of As₂O₃ in human leukemia HL-60 cells, as malondialdehyde (MDA) level was increased by increasing dosage of AA, and AA cotreated with As₂O₃ increased reactive oxygen species (ROS) generation11; AA enhanced antimyeloma effects of As₂O₃¹². Furthermore, it was demonstrated AA has preferable tolerance on recurrent/intractable myeloma13 and recurrent malignant tumor in lymphatic system¹⁴.

In this study, systems biology analysis was performed to investigate synergistic effects of As₂O₃ and AA in human osteosarcoma MG-63 cells, in order to further understand the synergistic mechanism of the two drugs, and figure out better drug combinative strategy for osteosarcoma.

Materials and Methods

Cell Line and Reagents

Human osteosarcoma MG-63 cells were from Institute of biochemistry and Cell Biology, Chinese Academy of Sciences (Shanghai, China). Fetal bovine serum (FBS) and Dulbecco's Modified Eagle Medium (DMEM) (high glucose) were purchased from Gibco (Carlsbad, CA, USA). AA and As₂O₃ powder were purchased from Beijing Dingguo Changsheng Biotechnology Co., Ltd (Beijing, China) and Beijing Doublecrane Pharmaceutical Co., Ltd (Beijing, China) respectively, and dissolved in phosphate buffered saline (PBS).

Cell Culture and Drug Administration

Human osteosarcoma MG-63 cells were cultured in the DMEM medium containing 10% FBS, 100 IU/mL penicillin, 100 μg/mL streptomycin at 37°C in 5% CO₂. Cells in logarithmic growth phase were planted as 30 000 cells/well in 24-well plates. As₂O₃ (1 μmol/L), AA (62.5 μmol/L) and combined drugs (1 μmol/L As₂O₃ plus 62.5 μmol/L AA) were administrated to the cells respectively for 72 h. Dynamic morphological characteristics were recorded every 2 h and analyzed by Cell-IQ continuous live cell imaging and analysis platform (Chip-man Technologies Ltd., Tampere, Finland).

Illumina Beadchip Assay

After the treatment, total RNA was extracted from cells using Trizol (Invitrogen, Carlsbad, CA, USA) reagent following the manufacturer's instruction. Reverse transcription, purification, hybridization, image reading and data analysis were performed using commercial kits and systems from Illumina (San Diego, CA, USA).

Identification of Synergic Drug Interaction Effects

To facilitate the identification of heterotypic interaction effects on global gene expression in mixed co-treated (1 µmol/L As₂O₃ plus 62.5 µmol/L AA) cells, we performed background adjustment and normalized the gene expression using Quantile normalization method (Supplement 1). After preprocessing, we averaged the biological replicates and then used mixture linear model to fit the normalization. To determine the contribution of each drug to the combined synergic effects of gene expression pattern in the linear regression model (Supplement 2), the expression levels of the mono-treated (1 µmol/L As₂O₃ or 62.5 µmol/L AA) cells are the predictors and the expression levels of the co-treated cells, the response. Interaction effects represented as gene expression changes. The ratio larger than 2 or less than 0.5 represents the relevant positive or negative interaction effect on the MG-63 cells from As_2O_3 or AA.

Gene Expression Decomposition Analysis

Distinct influences of varying magnitude within genes can be analyzed using SVD (singular value decomposition, Supplement 3) approach. SVD is an unsupervised algebric method that mathematically separates a gene expression matrix into a set of modes determined by the quanti-

tative composition of the data. Each mode is manifested in the data as a global expression component that influences the expression of each gene to a varying degree. SVD has also proved useful in linear modeling of gene expression, and gene classification, dimensional reduction and network modeling. Here, we used SVD method to deconvolute gene expression into component modes, which can reveal the significant gene sets those function in genetic or transcriptional regulation in co-treated (1 μ mol/L As₂O₃ plus 62.5 μ mol/L AA) cells or mono-type (1 μ mol/L As₂O₃ or 62.5 μ mol/L AA) cells.

Bioinformatic Analysis

The DAVID Bioinformatics Resources 6.7 (http://david.abcc.ncifcrf.gov/home.jsp) was used to make KEGG pathway annotations¹⁵. GO enrichment analysis was performed to reveal the relationships between the differential expressed genes (DEGs) and their possible regulatory functions.

Results

Ascorbic Acid Potentiates the Efficacy of As_2O_3 in MG-63 Cells

We compared the efficacy of combined use of AA (62.5 μ mol/L) and As₂O₃ (1 μ mol/L) with each monotherapy in osteosarcoma-derived MG-63 cell line. Within 32 h, both monotherapy (AA or As₂O₃) and combined therapy inhibited the growth of osteosarcoma cells. After 32 h, the inhibitory effect of combinational treatment (AA and As₂O₃) was greater than that of monotherapy (AA or As₂O₃, Figure 1).

Differential Expressed Genes (DEGs)

The results (without FDR correction) showed there were 2111 upregulated genes and 2181 downregulated genes in As₂O₃ monotreated cells, 286 upregulated genes and 584 downregulated genes in AA monotreated cells, and 2207 upregulated genes and 2323 downregulated genes in combinational treatment cells, respectively, compared with the control cells. After FDR correction, top 10 DEGs in the three groups were picked out as shown in Tables I to III. It was found FAT1 gene was significantly upregulated in all three groups, which is a promising drug target as an important tumor suppressor analogue^{16,17}. Meanwhile, HIST1H2BD gene was markedly downregulated in the As₂O₃ monotherapy group and the combined therapy group, which

was found to be upregulated in prostatic cancer¹⁸. Thus, we speculate these two genes might play critical roles in synergetic effects of AA and As_2O_3 , although the exact mechanism needs further investigation.

Genes Responsible for Synergistic Effects

Through drug combination data, we used linear mixture regression models to fit the normalized co-treated (As₂O₃ and AA) MG-63 expression profile. Using threshold of interaction effect computed from the fitted models, we captured 1987 genes, in which 730 positive-effected genes and 1257 negative-effected genes for MG-63 cells, respectively (Table IV). Based on previous knowledge, As₂O₃ and AA synergic interaction can double the cell therapy effects than As₂O₃ or AA individually treatment. Thus, the genes with positive or negative synergic effect in co-treated cells may function as key biomarkers in promotion of therapy effects.

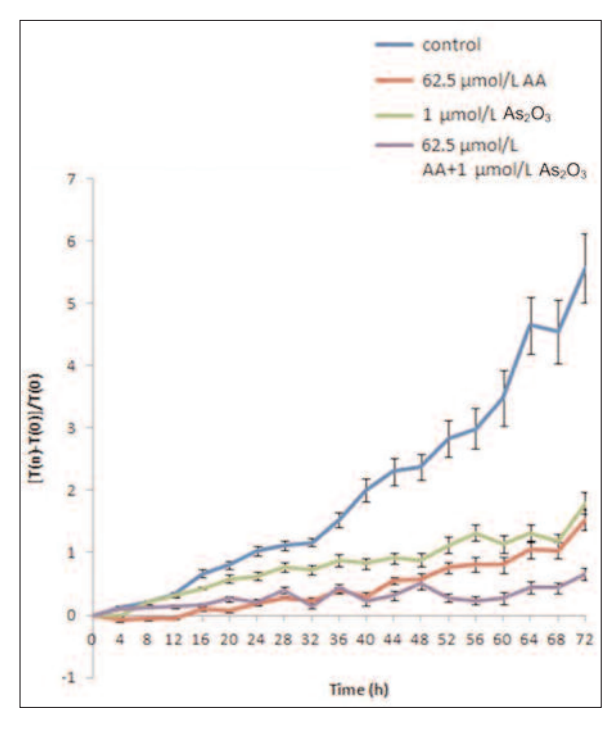


Figure 1. Effects of arsenic trioxide (As_2O_3) and ascorbic acid (AA) on growth rate of human osteosarcoma MG-63 cells. As_2O_3 (1 μ mol/L), AA (62.5 μ mol/L) and combined drugs (1 μ mol/L As_2O_3 plus 62.5 mol/L AA) were administrated to the cells respectively for 72 h. Dynamic morphological characteristics were recorded every 2 h and analyzed by Cell-IQ continuous live cell imaging and analysis platform. T(n) represents the cell number of the nth time point, and T(0) represents the cell number of the initial time point. Data were shown as mean \pm SD of at least three independent experiments.

Table I. Top 10 differential expression genes in ascorbic acid (62.5 μ mol/L AA) monotherapy MG-63 cells.

Differential expression genes	Average signal intensity of control cells	Average signal intensity of AA treated cells	Intensity difference scores (- downregulated)	Gene descriptions
GPN1	950	631	-52	GPN-loop GTPase 1
OGFOD1	1017	636	-51	2-oxoglutarate and iron-dependent oxygenase domain containing 1
VPS41	856	669	-51	Vacuolar protein sorting 41
C3orf75	305	192	-51	Chromosome 3 open reading frame 75
LOC286512	1171	701	-47	misc_RNA
TOMM7	9982	6734	-46	Translocase of outer mitochondrial membrane 7 homolog
PAPSS1	819	540	-46	3'-phosphoadenosine 5'-phosphosulfate synthase 1
LOC388275	1084	623	-45	Similar to heterogeneous nuclear ribonucleoprotein A1
C11orf54	319	232	-45	Chromosome 11 open reading frame 54
FBLN1	1216	2809	67	Fibulin 1
PFAS	160	379	57	Phosphoribosylformylglycinamidine synthase
GPC1	109	245	57	Glypican 1
GRN	239	911	57	Granulin
CMIP	286	924	53	c-Maf-inducing protein
FN3KRP	489	848	51	Fructosamine-3-kinase-related protein
AUTS2	162	351	51	Autism susceptibility candidate 2
HCFC1	310	1305	50	Fost cell factor C1
PRAMEF13	23	59	49	PRAME family member 13
FAT1	111	298	48	FAT tumor suppressor homolog 1

Table II. Top 10 differential expression genes in arsenic trioxide (1 μ mol/L AS₂O₃) monotherapy MG-63 cells.

Differential expression genes	Average signal intensity of control cells	Average signal intensity of AS ₂ O ₃ treated cells	Intensity difference scores (- downregulated)	Gene descriptions
HIST1H2BD	632	389	-17	Histone cluster 1, H2bd
C3orf75	305	192	-15	Chromosome 3 open reading frame 75 (C3orf75), mRNA.
GPN1	950	631	-15	GPN-loop GTPase 1
OGFOD1	1017	636	-15	2-oxoglutarate and iron-dependent oxygenase domain containing 1
VPS41	856	669	-15	Vacuolar protein sorting 41
C11orf54	319	232	-13	Chromosome 11 open reading frame 54
CTPS2	101	51	-13	CTP synthase II
LOC286512	1171	701	-13	misc_RNA
LOC388275	1084	623	-13	Similar to heterogeneous nuclear ribonucleoprotein A1
PAPSS1	819	540	-13	3'-phosphoadenosine 5'-phosphosulfate synthase 1
FAT1	111	298	13	FAT tumor suppressor homolog 1
PRAMEF13	23	59	14	PREDICTED: PRAME family member 13
HCFC1	310	1304	15	Host cell factor C1
AUTS2	162	351	15	Autism susceptibility candidate 2
CMIP	286	924	15	c-Maf-inducing protein
FN3KRP	489	848	15	Fructosamine-3-kinase-related protein
GPC1	109	245	17	Glypican 1
GRN	239	911	17	Granulin
PFAS	160	379	17	Phosphoribosylformylglycinamidine synthase
FBLN1	1216	2809	20	Fibulin 1

Table III. Top 10 differential expression genes in arsenic trioxide (1 μ mol/L AS_2O_3) and ascorbic acid (62.5 μ mol/L AA) combinational therapy MG-63 cells.

Differential expression genes	Average signal intensity of control cells	Average signal intensity of combinational therapy cells	Intensity difference scores (- downregulated)	Gene descriptions
OGFOD1	1017	697	-13	2-oxoglutarate and iron-dependent oxygenase domain containing 1
C11orf54	319	217	-13	Chromosome 11 open reading frame 54
PAPSS1	819	561	-13	3'-phosphoadenosine
rarss1	019	301	-13	5'-phosphoadenosme 5'-phosphosulfate synthase 1
GPN1	950	628	-11	GPN-loop GTPase 1 LOC28651
2	1171	688	-11 -10	misc_RNA
C3orf75	305	207	-10 -10	Chromosome 3 open reading frame 75
C301173	303	207	-10	(C3orf75), mRNA.LOC38827
5	1084	726	-10	Similar to heterogeneous nuclear ribonucleoprotein A1 HIST1H2B
D	632	381	-10	Histone cluster 1, H2bd
TOMM7	9982	6975	-9	TMranslocase of outer mitochondrial membrane 7 homolog
CTPS2	101	55	-8	CTP synthase II
FAT1	111	269	12	FAT tumor suppressor homolog 1
HCFC1	310	1400	13	Host cell factor C1
CNTNAP1	179	628	13	Contactin associated protein 1
COL1A2	2682	7539	13	Collagen, type I, alpha 2
GRN	239	878	13	Granulin
SOX13	45	118	13	SRY
FBLN1	1216	2892	14	Fibulin 1
CMIP	286	990	14	c-Maf-inducing protein
PFAS	160	359	14	Phosphoribosylformylglycinamidine synthase
PPRC1	232	491	14	Peroxisome proliferator-activated receptor gamma, coactivator-related 1

The Binary Transcriptional Regulatory Subnetworks

The organization of transcriptional regulation was analyzed using mode-state results and curated transcription factor-involved regulatory network. All available transcriptional regulations were downloaded from TRED database (http://ru-lai.cshl.eVC/TRED), which provides unique 6,797 TF-target regulation pairs with 121 transcription factors (TFs) and 2,992 target genes. The patterns

Table IV. As₂O₃-AA interaction effect and relevant gene set.

Probe_ID	InterEffect	Search_Key	ILMN_gene	Chromosome
ILMN 1657589	253.0755087	XM 927757.1	LOC644650	17
ILMN 1657147	88.5040932	XM 372447.3	LOC390282	12
ILMN 1735673	82.51870532	XM 927957.1	LOC644865	5
ILMN 1690863	81.11890942	NM 001001668.2	ZNF470	19
ILMN_1866286	52.79126142	Hs.574082	HS.574082	12
ILMN_1687792	51.3749073	XM_941994.1	DKFZP761O2018	
ILMN_1726936	51.21401449	XM_935249.1	LOC727735	17
ILMN_2325612	50.32299783	NM_181690.1	AKT3	1
ILMN_2197693	49.33697682	NM_004389.2	CTNNA2	2
ILMN_1737152	47.18364347	NM_001917.3	DAO	12
ILMN_1653347	45.95878893	XM_929661.1	LOC643697	20
ILMN_1674648	45.38198776	XM_943478.1	LOC338588	
ILMN_1710329	41.95442639	NM_016132.2	MYEF2	15
ILMN_1762573	41.01353356	NR_002161.1	LOC401630	Y

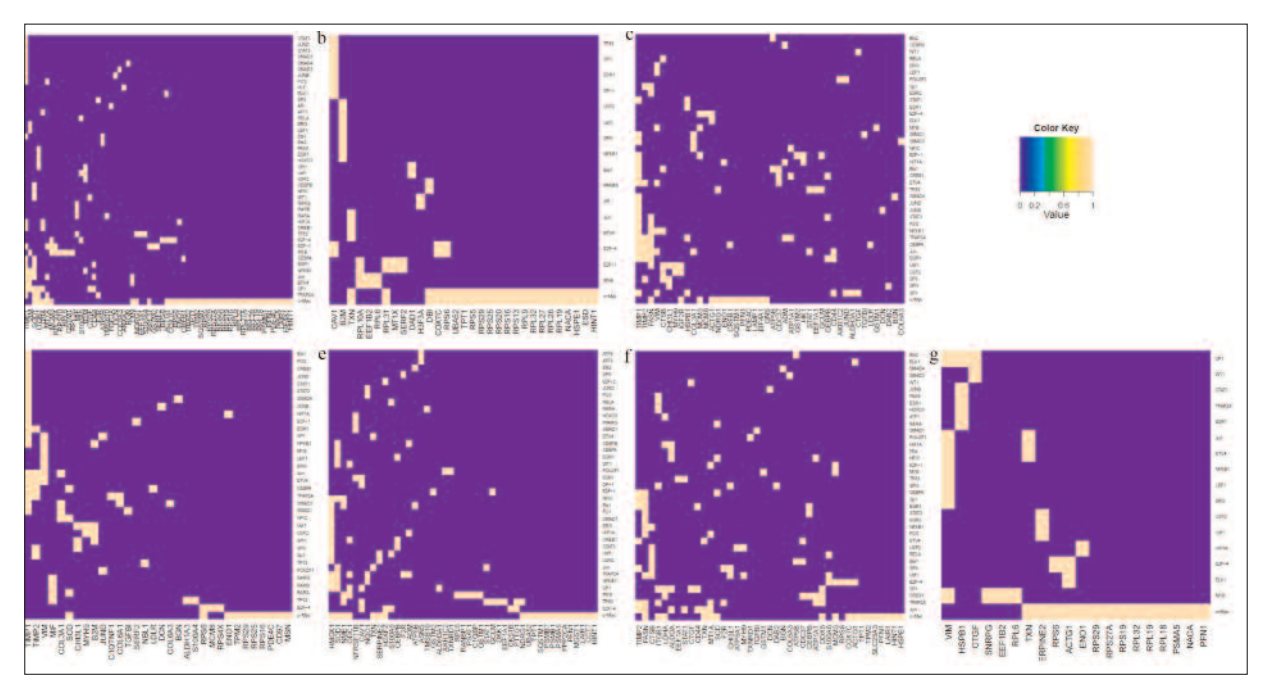


Figure 2. The patterns of transcription factor binding to gene-set members shown in the protein-DNA adjacency matrices. The binary heat maps, yellow means 1 = have interaction; blue means 0 = no interaction. Binary-valued adjacency matrices showed protein-DNA interactions for genes in SVD sets targeted by transcription factors. **A**, Mode-1-positive. **B**, Mode-2-negetive. **C**, Mode-2-positive. **D**, Mode-3-negetive. **E**, Mode-3-positive. **F**, Mode-4-negetive. **G**, Mode-4-positive.

of transcription factor binding to gene-set members are shown in the protein-DNA adjacency matrices (the binary heat maps, see Figure 2, yellow means 1 = have interaction; blue means 0 = no interaction). Binary-valued adjacency matrices showed protein-DNA interactions for genes in SVD sets targeted by transcription factors. Targeting patterns revealed that some subnetworks involve many genes bound by more than one of the TFs. Mode-state specific gene set may reveal condition specific subset. Each mode-state subnetwork summary is listed in Table V.

We obtained varies numbers of modes exhibited by the gene. The measured composite expression pattern of each gene in each condition is a summation of the contributions of the expression components. We intend to use SVD method to deconvolute the complex gene expression pattern and the results of each mode states correspond to condition-specific regulation patterns (Figure 3). The expression data set and the expression of every gene in each condition is decomposed into several components that are determined by SVD method. In contrast, previous traditional methods

Table V. The mode-state specific subnetwork summary.

	Como		Transcription	Torest			
Mode	Gene set num	Interactions	Transcription factors	Target num	Expected_Interaction	<i>p</i> value	Entropy
Mode-1-Positive	355	137	44	63	58.98295342	0.010297212	0.748323342
Mode-2-Positive	191	124	39	44	51.56796074	3.22E-05	0.798072578
Mode-2-Negative	204	45	17	31	23.31835712	0.753559417	0.7354161
Mode-3-Positive	149	105	39	45	47.05667002	0.02029479	0.811543893
Mode-3-Negative	163	81	36	32	37.79518168	0.099955717	0.799203629
Mode-4-Positive	153	38	17	20	19.41225088	0.552860037	0.780226116
Mode-4-Negative	142	111	39	41	48.73416409	0.002743291	0.79221499

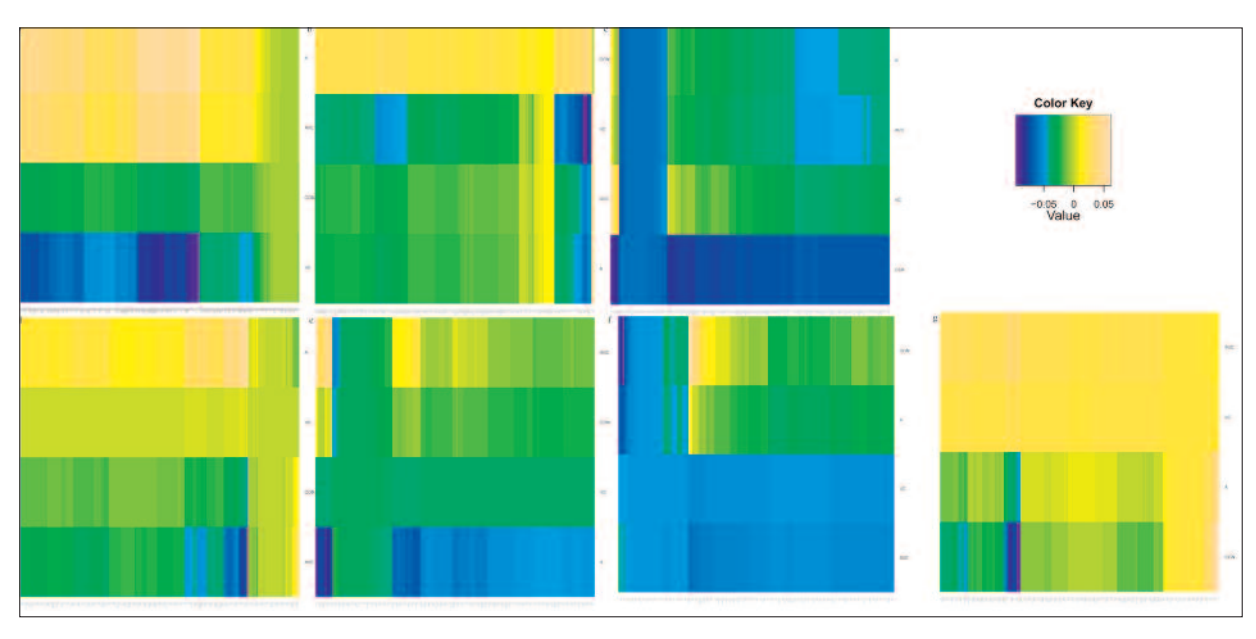


Figure 3. The expression data set and the expression of every gene in each condition is decomposed into several components that are determined by SVD method. We intend to use SVD method to deconvolute the complex gene expression pattern and the results of each mode states correspond to condition-specific regulation patterns. The binary heat maps, yellow means 1 = have interaction; blue means 0 = no interaction. **A**, Mode-1-positive. **B**, Mode-2-negetive. **C**, Mode-2-positive. **D**, Mode-3-negetive. **E**, Mode-3-positive. **F**, Mode-4-negetive. **G**, Mode-4-positive.

that based on clustering method without decomposition cannot isolate the overlapping regulatory influences of varying magnitude.

Go & Pathway

We made KEGG pathway annotations of 1987 DEGs in combined therapy MG-63 cells using DAVID Bioinformatics Resources, and found these genes mainly gathered in pathways related with tight junction, long-term depression and arachidonic acid metabolism (Table VI). Additionally, GO enrichment analysis showed the DEGs gathered in the gene ontologies including tight junction, occluding junc-

tion, cell junction (Table VII). The DEGs gathering in tight junction pathway were shown in Figure 4 as an example.

Discussion

Current researches have determined low dose As_2O_3 mainly inhibits tumor cell proliferation, while high dose As_2O_3 has cytotoxicity, not only on leukemia, but also on solid tumor. Considering severe side effects caused by high dose As_2O_3 , drug combination is thought to be a preferable approach. In this study, we found

Table VI. KEGG pathway annotations of 1987 differential expression genes in combined therapy MG-63 cells.

Term	Gene number	%	<i>p</i> value	Genes
hsa04530: Tight junction	16	1.381	0.001	CLDN8, PARD6B, CLDN9,MYH3, CRB3, AMOTL1, CTNNB1, CTNNA2, MYL9, PRKCQ, IGSF5, EPB41L1, TJP2, AKT3, LOC284620, AKT2
hsa04730: Long-term depression	8	0.690	0.041	GNAZ, GRM5, PLCB4, JMJD7, GNA12, RYR1, PLA2G2C, GRIA3
hsa00590: Arachidonic acid metabolism	7	0.604	0.045	PTGIS, CYP2C18, ALOX15B, JMJD7, PLA2G2C, GGT1, ALOX5

Table VII. GO enrichment analysis of 1987 differential expression genes in combined therapy MG-63 cells.

		_			
Classification	Term	Gene number	%	<i>p</i> value	Genes
GOTERM_BP_FAT	GO:0030182 neuron differentiation	38	3.279	0.001	NRP2, CCKAR, LOC100129095, CLU, SOX2, ONECUT2, L1CAM, PAX3, RORA, PAX2, NR2E1, RTN1, HOXA1, ALDH1A2, ROBO1, ANK3, LHX5, GF11, TLX3, HSN2, APC, SCLT1, PARD6B, UCN, KLK8, NRXN3, BAIAP2, TGFBR1, PTPRR, LOC344593, CTNNA2, AMIGO1, PRKCQ, PSEN1, OPHN1, CNTN4, CLN8, KALRN
GOTERM_CC_FAT	GO:0005923 tight junction	12	1.035	0.001	CLDN8, IGSF5, PARD6B, CLDN9, LOC283999, CRB3, AMOT, ESAM, AMOTL1, TJP2, LOC284620, APC
GOTERM_CC_FAT	GO:0070160 occluding junction	12	1.035	0.001	CLDN8, IGSF5, PARD6B, CLDN9, LOC283999, CRB3, AMOT, ESAM, AMOTL1, TJP2, LOC284620, APC
GOTERM_CC_FAT	GO:0043296 apical junction complex	14	1.208	0.001	CLDN8, PARD6B, CLDN9, CRB3, AMOTL1, CTNNB1, IGSF5, LOC283999, AMOT, DSP, ESAM, TJP2, APC, LOC284620
SP_PIR_KEYWORD S	Cell junction	35	3.020	0.001	CLDN8, CLDN9, GABRB3, GABRB2, NEDD9, SYT7, CTNNB1, COL17A1, CHRNA9, SYN1, SYN3, RASGRP2, ESAM, CHRNA1, CHRNA3, LOC284620, APC, NPHP1, PARD6B, TMEM204, CRB3, GRIA3, SSPN, CTNNA2, DNMBP, SLC17A7, IGSF5, KLHL17, RAPSN, DOK7, OPHN1, AMOT, DSP, TJP2, CHRNA10
GOTERM_CC_FAT	GO:0016327 apicolateral plasma membrane	14	1.208	0.001	CLDN8, PARD6B, CLDN9, CRB3, AMOTL1, CTNNB1, IGSF5, LOC283999, AMOT, DSP, ESAM, TJP2, APC, LOC284620
GOTERM_BP_FAT	GO:0048858 cell projection morphogenesis	24	2.071	0.002	NRP2, PARD6B, CCKAR, KLK8, LOC100129095, KIF3A, NRXN3, BAIAP2, CLU, ONECUT2, LOC344593, RPGRIP1L, L1CAM, PAX2, NR2E1, CTNNA2, AMIGO1, HOXA1, ROBO1, ANK3, OPHN1, CNTN4, KALRN, APC
GOTERM_BP_FAT	GO:0032990 cell part morphogenesis	24	2.071	0.003	NRP2, PARD6B, CCKAR, KLK8, LOC100129095, KIF3A, NRXN3, BAIAP2, CLU, ONECUT2, LOC344593, RPGRIP1L, L1CAM, PAX2, NR2E1, CTNNA2, AMIGO1, HOXA1, ROBO1, ANK3, OPHN1, CNTN4, KALRN, APC

Table continued

AA potentiates the efficacy of As₂O₃ in MG-63 cells. Global gene expression analysis figured out the synergic effects on gene expression mode in MG-63 cells, and found the DEGs in

monotherapy and combined therapy cells. FAT1 gene was significantly upregulated in all three groups, which is a promising drug target as an important tumor suppressor analogue^{16,17}.

Table VII *(Continued).* GO enrichment analysis of 1987 differential expression genes in combined therapy MG-63 cells.

Classification	Term	Gene number	%	<i>p</i> value	Genes
GOTERM_CC_FAT	GO:0030054 cell junction	40	3.451	0.003	CLDN8, CLDN9, GABRB3, GABRB2, NEDD9, SYT7, AMOTL1, CTNNB1, COL17A1, CHRNA9, SYN1, ARPC2, SYN3, RASGRP2, ESAM, CHRNA1, CHRNA3, LOC284620, APC, NPHP1, PARD6B, TMEM204, ARHGEF7, CRB3, GRIA3, LIG4, SSPN, CTNNA2, KLHL17, RAPSN, LOC283999, DOKP, OPHN1, AMOT, DSP, TJP2,
GOTERM_BP_FAT	GO:0048812 neuron projection morphogenesis	21	1.812	0.003	CHRNA10 NRP2, PARD6B, CCKAR, KLK8, LOC100129095, NRXN3, BAIAP2, CLU, LOC344593, L1CAM, PAX2, NR2E1, CTNNA2, AMIGO1, HOXA1, ROBO1, ANK3, OPHN1, CNTN4, APC, KALRN
GOTERM_BP_FAT	GO:0002252 immune effector process	15	1.294	0.005	POLL, CPLX2, CR1, C6, CLU, MY01F, LIG4, C4BPA, CD74, FOXP1, C1QA, LAT, ABCC9, MLL5, PMS2CL
GOTERM_BP_FAT	GO:0007409 axonogenesis	19	1.639	0.006	NRP2, PARD6B, CCKAR, LOC100129095, NRXN3, BIAP2, LOC344593, L1CAM, PAX2, NR2E1, CTNNA2, AMIGO1, HOXA1, ROBO1, ANK3, OPHN1, CNTN4, APC, KALRN
SP_PIR_KEYWORD S	Ionic channel	27	2.330	0.006	GABRB3, SCN3A, GABRB2, KCNAB1, ANO1, KCNA5, KCNIP1, KCNK12, KCNJ14, KCNMB2, KCNIP3, BEST4, CHRNA9, TRPV5, TRPV4, CHRNA1, CHRNA3, TRPM8, TMEM38A, CACNG4, GRIA3, KCNV2, CATSPER2, RYR1, CACNA1C,
GOTERM_BP_FAT	GO:0030030 cell projection organization	30	2.588	0.006	KCNH2, CHRNA10 NRP2, CCKAR, LOC100129095, PDGFA, CLU, ONECUT2, ITGB4, L1CAM, PAX2, NR2E1, HOXA1, C19ORF20, ROBO1, ANK3, TEKT4, APC, KLF5, PARD6B, KLK8, UCN, KIF3A, NRXN3, BAIAP2, RPGRIP1L, LOC344593, CTNNA2, AMIGO1, OPHN1, CNTN4, KALRN
GOTERM_MF_FAT	GO:0005261 cation channel activity	24	2.071	0.006	TRPM8, SCN3A, KCNAB1, TMEM38A, CACNG4, KCNA5, KCNIP1, KCNV2, FKBP1B, KCNK12, KCNJ14, KCNIP3, KCNMB2, ABCC9, CHRNA9, CATSPER2, TRPV5, RYR1, TRPV4, CHRNA1, CACNA1C, KCNH2, CHRNA10, CHRNA3
GOTERM_BP_FAT	GO:0006836 neurotransmitter transport	11	0.949	0.006	SLC17A7, CPLX2, PSEN1, SYN1, NRXN3, SLC6A12, SYN3, SERPINB7, SLC6A16, SLC6A19, CLN8

Table continued

Table VII *(Continued).* GO enrichment analysis of 1987 differential expression genes in combined therapy MG-63 cells.

Classification	Term	Gene number	%	<i>p</i> value	Genes
Classification	Term	Hullibei	70	p value	Genes
	GO:0000904 cell morphogenesis involved in differentiation	22	1.898	0.007	NRP2, PARD6B, CCKAR, NOG, LOC100129095, CRYAA, NRXN3, BAIAP2, LOC344593, L1CAM, PAX2, NR2E1, CTNNB1, CTNNA2, AMIGO1, HOXA1, ROBO1, ANK3, OPHN1, CNTN4, APC, KALRN
SP_PIR_KEYWORD S	Calcium transport	11	0.949	0.008	SLC8A3, ATP2B1, SLC24A4, CHRNA9, CATSPER2, RYR1, TRPV5, CACNG4, TRPV4, CACNA1C, CHRNA10
GOTERM_BP_FAT	GO:0002443 leukocyte mediated immunity	11	0.949	0.008	C1QA, LAT, CR1, CPLX2, MLL5, C6, CLU, MYO1F, LIG4, C4BPA, CD74
UP_SEQ_FEATURE	Topological domain: Extracellular	158	13.632	0.009	SLC8A3, C200RF107, IL9R, GPR125, GABRB3, GABRB2, LRTM1, C60RF25, OR1J1, DLK2, L1CAM, GGT1, TSPAN8, ATP2B1, SEZ6L2, OR4D2, FAM171B, CHRNA9, CLEC4E, OR51T1, ROBO1, CLEC4A, CHRNA1, INSR, PQLC2, CHRNA3, TMEM204, GPR135, PTPRR, OR4M2, UNC5CL, PTPRT, C10RF210, PKHD1L1, SSPN, CRHR2, IGSF5, CCR6, CATSPER2, ATP9A, CD164L2, TMPRSS11B, CD200R1L, KIR3DL1, GPR146, ENPP6, SLC2A11, CYSLTR2, RTP1, TMIGD1, ITGB4, ITGB3, GPR143, CD74, KCNMB2, MIA3, RNFT2, BAI2, ADAM32, OR2T6, ADAM33, T-SP1, CSF1R, ADAM23, TGFBR1, SLC6A12, CRB3, SLC6A16, AQP10, SLC6A19, PORCN, GUCY2D, TIGIT, LAT, RNF150, THSD1, ADRA1A, SYT15, CACNA1C, SLC5A10, NRP2, CLDN8, SLC45A2, CCKAR, LOC100129095, CLDN9, PCDHA9, NRG3, TACR3, OR2A42, ANO1, OR4K17, OR1N1, CDCP1, PCDHA1, K CNJ14, SDC3, CCRL2, VN1R2, SLC24A4, EVI2A, SMAGP, TRPV5, TRPV4, ESAM, SLC22A6, CSF2RA, LRC37B, RAMP2, PTGER3, TRPM8, NRXN3, SDK2, RXFP2, PCDHB2, OR10J1, LDLRAD2, GRM5, AMIGO1, KIAA1161, TAS2R14, SEMA4G, ALG10B, SGCD, OR4N2, KIR2DL5B, SLC39A13, GPR64, TNFRSF4, CLEC10A, BEST4, APLP1, COL17A1, PRRG4, CDH9, PCDHB16, SHISA4, TNFRSF19, LOC284620, OR1B1,
SP_PIR_KEYWORD S	Tight junction	9	0.777	0.009	CR1, PTPRE, GFRAL, LRRN2, ATRN, CD1C, TMPRSS7, GRIA3, TNFSF9, CD180 SLC17A7, ABCC9, KREMEN2, CDON, CDH19, CD302, CHRNA10, ABCC6 CLDN8, IGSF5, PARD6B, CLDN9,
SP_PIR_KEYWORD S		9	0.777	0.009	CRB3, AMOT, ESAM, TJP2, LOC284620 CLDN8, IGSF5, PARD6B, CLDN9, CRB3, AMOT, ESAM, TJP2, LOC284620

Meanwhile, HIST1H2BD gene was markedly downregulated in the As_2O_3 monotherapy group and the combined therapy group, which was found to be upregulated in prostatic cancer¹⁸.

These two genes might play critical roles in synergetic effects of AA and As₂O₃, although the exact mechanism needs further investigation.

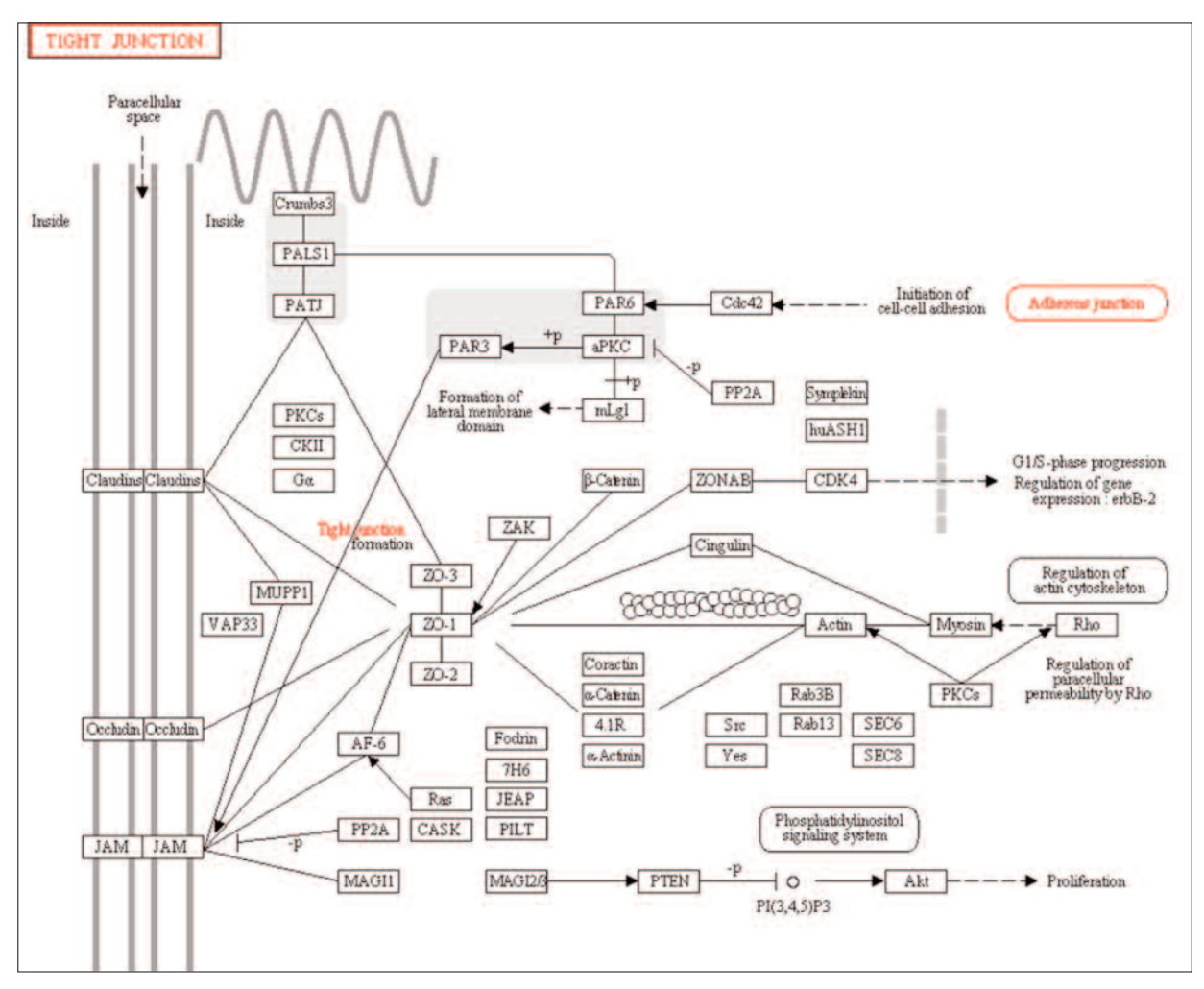


Figure 4. Differential expression genes in combined therapy (1 μ mol/L As_2O_3 plus 62.5 μ mol/L AA) MG-63 cells gathering in tight junction pathways.

KEGG pathway analysis showed many differential expression genes were related with tight junction, and GO analysis also indicated that differential expression genes in the combined therapy cells gathered in occluding junction, apical junction complex, cell junction, and tight junction. These results suggested AA and As₂O₃ cotreated might change the cell junctions, induce morphological transformation, promote cell differentiation, and finally cause cell apoptosis.

Binary-valued adjacency matrices showed protein-DNA interactions for genes in SVD sets targeted by TFs. Targeting patterns revealed that some subnetworks involve many genes bound by more than one of the TFs. Mode-state specific gene set may reveal condition specific subset. We obtained varies numbers of modes exhibited by the gene. The measured composite expression

pattern of each gene in each condition is a summation of the contributions of the expression components. We also used SVD method to deconvolute the complex gene expression pattern and the results of each mode states correspond to condition-specific regulation patterns.

Conclusions

AA potentiates the efficacy of As₂O₃ in MG-63 cells. Systems biology analysis showed the synergic effect on the DEGs, and provided effect modes as well.

Conflict of Interest

The Authors declare that there are no conflicts of interest.

References

- TAN JZ, SCHLICHT SM, POWELL GJ, THOMAS D, SLAVIN JL, SMITH PJ, CHOONG PF. Multidisciplinary approach to diagnosis and management of osteosarcoma--a review of the St Vincent's Hospital experience. Int Semin Surg Oncol 2006; 3: 38.
- MARCOVE RC, MIKE V, HAJEK JV, LEVIN AG, HUTTER RV. Osteogenic sarcoma under the age of twentyone. A review of one hundred and forty-five operative cases. J Bone Joint Surg Am 1970; 52: 411-423
- Anninga JK, Gelderblom H, Fiocco M, Kroep JR, Taminiau AH, Hogendoorn PC, Egeler RM. Chemotherapeutic adjuvant treatment for osteosarcoma: where do we stand? Eur J Cancer 2011; 47: 2431-2445.
- KRITHARIS A, BRADLEY TP, BUDMAN DR. The evolving use of arsenic in pharmacotherapy of malignant disease. Ann Hematol 2013; 92: 719-730.
- LALLEMAND-BREITENBACH V, ZHU J, CHEN Z, DE THE H. Curing APL through PML/RARA degradation by As2O3. Trends Mol Med 2012; 18: 36-42.
- ZHANG T, WANG SS, HONG L, WANG XL, QI QH. Arsenic trioxide induces apoptosis of rat hepatocellular carcinoma cells in vivo. J Exp Clin Cancer Res 2003; 22: 61-68.
- FANG C, CHEN ZG, YU AX, ZHU SB. Inhibitory effects of arsenic trioxide on osteosarcoma and diploid cell lines. Chinese J Exp Surg 2003; 20: 446-447.
- REHMAN K, AKASH MS, NARANMANDURA H. Doubleedged effects of arsenic compounds: anticancer and carcinogenic effects. Curr Drug Metab 2013; 14: 1029-1041.
- YEDJOU CG, ROGERS C, BROWN E, TCHOUNWOU PB. Differential effect of ascorbic acid and n-acetyl-Lcysteine on arsenic trioxide-mediated oxidative stress in human leukemia (HL-60) cells. J Biochem Mol Toxicol 2008; 22: 85-92.
- GE FM, BAI QX, LIU YX, HUANG GS. Ascorbic acid enhances apoptosis of multiple myeloma RPMI 8226 cells induced by arsenic trioxide. Tumor 2006; 4: 331-334.

- Guo W, Tang XD, Tang S, Yang Y. [Preliminary report of combination chemotherapy including Arsenic trioxide for stage III osteosarcoma and Ewing sarcoma]. Zhonghua Wai Ke Za Zhi 2006; 44: 805-808.
- 12) CAMPBELL RA, SANCHEZ E, STEINBERG JA, BARITAKI S, GORDON M, WANG C, SHALITIN D, CHEN H, PANG S, BONAVIDA B, SAID J, BERENSON JR. Antimyeloma effects of arsenic trioxide are enhanced by melphalan, bortezomib and ascorbic acid. Br J Haematol 2007; 138: 467-478.
- 13) BERENSON JR, HILGER JD, YELLIN O, BOCCIA RV, MATOUS J, DRESSLER K, GHAZAL HH, JAMSHED S, KINGSLEY EC, HARB WA, NOGA SJ, NASSIR Y, SWIFT RA, VESCIO R. A phase 1/2 study of oral panobinostat combined with melphalan for patients with relapsed or refractory multiple myeloma. Ann Hematol 2014; 93: 89-98.
- 14) CHANG JE, VOORHEES PM, KOLESAR JM, AHUJA HG, SANCHEZ FA, RODRIGUEZ GA, KIM K, WERNDLI J, BAILEY HH, KAHL BS. Phase II study of arsenic trioxide and ascorbic acid for relapsed or refractory lymphoid malignancies: a Wisconsin Oncology Network study. Hematol Oncol 2009; 27: 11-16.
- HUANG DA W, SHERMAN BT, LEMPICKI RA. Systematic and integrative analysis of large gene lists using DAVID bioinformatics resources. Nat Protoc 2009; 4: 44-57.
- KATOH Y, KATOH M. Comparative integromics on FAT1, FAT2, FAT3 and FAT4. Int J Mol Med 2006; 18: 523-528.
- 17) Lu Y, Nie D, Witt WT, Chen Q, Shen M, Xie H, Lai L, Dai Y, Zhang J. Expression of the fat-1 gene diminishes prostate cancer growth in vivo through enhancing apoptosis and inhibiting GSK-3 beta phosphorylation. Mol Cancer Ther 2008; 7: 3203-3211.
- LIN HP, JIANG SS, CHUU CP. Caffeic acid phenethyl ester causes p21 induction, Akt signaling reduction, and growth inhibition in PC-3 human prostate cancer cells. PLoS One 2012; 7: e31286.
- Huang da W, Sherman BT, Lempicki RA. Bioinformatics enrichment tools: paths toward the comprehensive functional analysis of large gene lists. Nucleic Acids Res 2009; 37: 1-13.